CSIRO PUBLISHING

International Journal of Wildland Fire **2008**, *17*, 638–649 www.publish.csiro.au/journals/ijwf

Quantifying parametric uncertainty in the Rothermel model

Edwin Jimenez[A], *M. Yousuff Hussaini*[A,C] *and Scott Goodrick*[B]

[A]School of Computational Science, Florida State University, Dirac Science Library, Tallahassee, FL 32306, USA.

[B]USDA Forest Service Center for Forest Disturbance Science, 320 Green Street, Athens, GA 30602, USA.

[C]Corresponding author. Email: myh@scs.fsu.edu

Abstract. The purpose of the present work is to quantify parametric uncertainty in the Rothermel wildland fire spread model (implemented in software such as *BehavePlus3* and *FARSITE*), which is undoubtedly among the most widely used fire spread models in the United States. This model consists of a non-linear system of equations that relates environmental variables (input parameter groups) such as fuel type, fuel moisture, terrain, and wind to describe the fire environment. This model predicts important fire quantities (output parameters) such as the head rate of spread, spread direction, effective wind speed, and fireline intensity. The proposed method, which we call sensitivity derivative enhanced sampling, exploits sensitivity derivative information to accelerate the convergence of the classical Monte Carlo method. Coupled with traditional variance reduction procedures, it offers up to two orders of magnitude acceleration in convergence, which implies that two orders of magnitude fewer samples are required for a given level of accuracy. Thus, it provides an efficient method to quantify the impact of input uncertainties on the output parameters.

Introduction

One of the primary goals of wildland fire management is to minimise the negative impact of fire on property and society through the application of scientific research. To meet this goal, fire researchers employ a variety of tools such as satellite imagery, experiments and fire danger indices, as well as mathematical models. A typical mathematical fire behaviour model usually consists of a set of non-linear equations. These equations, which are most commonly non-linear algebraic equations or non-linear differential equations, describe the interaction of the various environmental variables and can be used to predict valuable information such as the maximum rate of spread and spread direction.

Fire models typically fall into one or more of the following categories. They are either physics-based, or derived empirically, or constructed from statistical considerations. A fire model that is physics-based uses physical principles such as conservation of energy, mass and momentum to derive a formula for the rate of spread and other quantities of interest; see Weber (2001) and the references therein for an in-depth discussion. It is also possible to use a statistical description of test fires to predict fire behaviour occurring under similar conditions. The McArthur models (McArthur 1966) used for grassland and forest fires in Australia are one such example. Finally, laboratory experiments can be performed to empirically determine quantities such as the propagating flux, which can, in turn, be used to obtain an expression for the rate of spread. The Rothermel model (Rothermel 1972), a fire spread model that spans the physical and empirical classes, is perhaps the best-known model in the United States and although more recent models include a wider range of fire phenomena, it is still in wide use today.

Not all fire models, however, can be employed as efficient fire prediction tools. Some of the more complex models, which couple atmospheric and fire behaviour effects, for instance, are currently too computationally expensive to serve as viable real-time prediction tools. These complex models, nevertheless, assist researchers in gaining a more profound understanding of fire behaviour.

The Rothermel fire spread model

The Rothermel wildland fire spread model (Rothermel 1972) was one of the first models to describe the fire environment through equations derived, for the most part, from thermodynamic principles. The term fire behaviour is used to describe physical characteristics of a fire such as its rate of spread, fire line intensity, flame length, etc. The ensemble of fuels, terrain, and weather is usually referred to as the fire environment. In North America, where forests and grasslands provide an abundant source of wildland fuel, wildland fires are of particular interest. Wildland fuels are fuels that consist primarily of vegetation, both live and dead, but may include organic layers within the soil. A surface fire, the type of fire the Rothermel model was developed for, spreads through a layer of contiguous fuel extending from the ground up to approximately 2 metres. This definition differentiates a surface fire from one moving through the tree canopies (crown fires) or one burning through organic soil material (ground fire). Although this model uses the principle of conservation of energy to derive an equation for the rate of spread, no distinction is made between the different modes of heat transfer. The propagating flux ξ, which is used to extract an equation for the rate of spread, is determined empirically. Thus, the Rothermel model is sometimes referred to as

 10.1071/WF07070 1049-8001/08/050638

a semi-empirical model to emphasise its hybrid physical and empirical nature.

The Rothermel model groups input parameters into four main categories: fuel type, fuel moisture, topography, and weather. One simplifying assumption regarding the fuels is that for a small area and short time periods, the fuels are taken to be homogeneous. The fuel parameter groups include fuel particle properties such as fuel loading, fuel moisture content, and surface-area-to-volume ratio. The remaining topography and wind groups account for the slope, aspect, relative humidity, wind speed, etc. The burning layer, composed of the conglomerate of fuel parameters, is referred to as the fuel bed or fuel model.

The output variables we shall consider are the *rate of spread* (*ros* in $\mathrm{m\,s^{-1}}$), the *direction of maximum spread* (*sdr* in degrees), and the *effective wind speed* (*efw* in $\mathrm{m\,s^{-1}}$). Other quantities such as fire line intensity, heat release per unit area, and flame length can also be derived.

There are certain fire behaviour aspects that the Rothermel model does not take into account, however. The model's assumptions of steady-state and spatial homogeneity preclude its application to transitory events such as crown fire initiation or spotting. The addition of *ad hoc* wind and slope factors intended to modify the rate of spread also warrant deeper scrutiny.

Despite its limitations, the Rothermel model has enjoyed widespread success and it is currently employed in software such as in *BehavePlus3* and *FARSITE*. Using either default fuel models or user-defined input parameters, *BehavePlus3* can calculate output variables such as the rate of spread and spread direction. *FARSITE* (Finney 1998) is a fire growth simulation system that uses a combination of models to simulate surface fires along with other phenomena such as crown fires, spotting, and post-frontal combustion. *FARSITE* requires the use of a geographic information system (GIS) database to obtain spatial landscape information. Using a fire spread model in conjunction with estimated evacuation times, Cova *et al*. (2005) have also exploited the use of GIS to develop a method similar to hurricane warnings to set trigger points used in evacuation.

Parametric uncertainty in fire spread models

To properly use a fire model, it is essential to understand its limitations and scope of applicability. However, even when fire models are used adequately, discrepancies between the observed phenomena and model results are inevitable as models are derived under idealised conditions. Model errors can result from several factors including inadequate physical description, numerical errors, and parametric uncertainty (Walters and Huyse 2002). In the present work, we concentrate our efforts solely on those errors originating from parametric uncertainty. In order to adequately describe the impact of parametric uncertainty, it is important to quantify the uncertainty mathematically. As the value of an input parameter is seldom known exactly, a common approach (and the one we will pursue) is to assign it a mean value and an associated probability density function. The standard deviation can then be taken as a measure of the uncertainty in the parameter value. The impact of parametric uncertainty on the results can then be estimated using, for instance, a Monte Carlo simulation or a moments method.

Sometimes uncertainty in an input parameter is not only a consequence of the intrinsic complexity of the phenomena being modelled. Instead, uncertainties may be the inevitable by-products of economic and efficiency constraints. For example, it may be expensive or intractable to measure fuel data directly, as in the case of a large area.

However, it is not always necessary to concern ourselves with the uncertainty associated with every single parameter. A sensitivity analysis can help us identify the input parameters that have the greatest influence on output variables (Saltelli *et al*. 2004). Those parameters that have only a marginal impact on the quantities of interest can be assigned constant characteristic values to reduce computational demands. Having identified the major sources of error due to parametric uncertainty, the next step involves taking measures to improve the reliability of our predictions. Fujioka (2002) proposes a methodology to analyse the error in a two-dimensional fire spread simulation that can also be used as a correction tool when it is coupled with updated information.

Problem formulation

We will focus on quantifying the impact and propagation of parametric uncertainty only on the following output variables: the *rate of spread* (*ros* in $\mathrm{m\,s^{-1}}$), the *direction of maximum spread* (*sdr* in degrees), and the *effective wind speed* (*efw* in $\mathrm{m\,s^{-1}}$). Using the same notation as in Bachmann (2001), the Rothermel steady-state rate of spread equation can be written as:

$$ros = \frac{I_R \xi (1 + \Phi_c)}{\rho_b \varepsilon Q_{ig}} \tag{1}$$

where I_R is the reaction intensity, ξ is the propagating flux ratio, ρ_b is the oven-dry bulk density, ε is the effective heating number, and Q_{ig} is the heat of pre-ignition. If Φ_w and Φ_s are the wind and slope correction factors, respectively, then the combined slope and wind factor Φ_c is given by:

$$\Phi_c = \sqrt{[\Phi_s + \Phi_w \cos(\theta)]^2 + [\Phi_w \sin(\theta)]^2}$$

Here θ is the angle between the upslope direction and the direction where the wind is blowing to. The spread direction and the effective wind speed are given by:

$$sdr = \arcsin\left[\frac{\Phi_w \sin(\theta)}{\Phi_c}\right] \text{ and}$$

$$efw = \frac{1}{196.85}\left[\frac{\Phi_c}{C(\sigma)(\beta/\beta_{opt})^{-E(\sigma)}}\right]^{1/B(\sigma)}$$

respectively. B, C and E are functions of the characteristic surface-area-to-volume ratio σ, β is the mean packing ratio, and β_{opt} denotes the optimal packing ratio; the full set of equations as well as their derivatives can be found in Bachmann (2001).

The output variables depend on the following parameters: fuel loading $w0_{d1}, w0_{d2}, w0_{d3}, w0_{lh}, w0_{lw}$ (in $\mathrm{kg\,m^{-1}}$), surface-area-to-volume ratio $sv_{d1}, sv_{d2}, sv_{d3}, sv_{lh}, sv_{lw}$ (in $\mathrm{m^2\,m^{-3}}$), fuel moisture content $m_{d1}, m_{d2}, m_{d3}, m_{lh}, m_{lw}$ (in %), fuel bed depth d (in m), wind speed wsp (in $\mathrm{m\,s^{-1}}$), wind direction θ (in degrees), aspect ratio asp (in degrees), and slope slp (in degrees). The subscripts $d1$, $d2$, $d3$, lh, lw denote the size classes traditionally used to categorise the different fuel moisture time-lag classes (Deeming *et al*. 1978): dead fuel, 0–0.6 cm; dead fuel,

0.6–2.5 cm; dead fuel, 2.5–7.5 cm; live herbaceous fuel; and live woody fuel, respectively. Throughout the present paper, we assume that those parameters that are not held constant follow a normal distribution with a given mean and standard deviation.

The methodology we will use to quantify the propagation and impact of parametric uncertainty will be to employ an efficient Monte Carlo method. The Monte Carlo convergence rate is accelerated through the use of a sensitivity derivative enhanced sampling method that exploits derivative information of the output functions with respect to the input parameters to make more judicious use of the samples generated in a simulation. We estimate the mean and standard deviation of the output variables using a traditional Monte Carlo method as well as with the sensitivity derivative enhanced sampling method (SDES), and compare the advantages of SDES over the Monte Carlo method via improvement ratios and timing performance. The distributions of output variables will also be generated. It should be noted that the computation of the required sensitivity derivatives accounts for only a fraction of the total cost of a simulation; these can be easily extracted using, for instance, an automatic differentiation package.

Numerical method

To investigate the propagation and impact of input variable uncertainties, Bachmann and Allgower (2002) used a first-order Taylor method in place of a fully-fledged Monte Carlo simulation to avoid the prohibitive computational expense incurred through a direct application of the classical Monte Carlo method. Indeed, because of its slow convergence rate and the costly generation of correlated input variables in the multivariate case, Monte Carlo methods are usually reserved to establish a reference against which other methods are compared. However, by identifying and generating stochastic versions of only those parameters to which the output variables are most sensitive and at the same time improving the convergence characteristics of traditional Monte Carlo methods, it is possible to perform simulations utilising the original model to capture the more intricate behaviour that a low-order approximation, such as a first-order Taylor expansion, might otherwise sacrifice. The modified Monte Carlo method we describe below is a step towards this goal.

Although Monte Carlo methods have long been popular in part because they are simple to implement and use the underlying model as a 'black box,' their slow convergence rate often proves to be too inefficient especially when multiple simulations are required. A common approach to improve the convergence rate, which is known to be proportional to the variance of the objective function, is to reduce the variance via a suitable reformulation of the problem. Variants of this approach encompass a large class of methods collectively known as variance-reduction methods. The SDES method, which we describe below, is a variance-reduction method that has already been employed with success in fields such as optimal control (Cao *et al*. 2003, 2004) and computational fluid dynamics (Mathelin *et al*. 2004). In this section, we review the theory underlying the method (our discussion closely follows Cao *et al*. 2004, 2006). The methods we shall employ are described in their proper mathematical setting, but for the reader who is unfamiliar with some of the concepts discussed below, the textbooks of Ross (1997) and Shiryayev (1984) should elucidate some of the mathematical details that are omitted.

Monte Carlo method

Given a random variable X with finite expectation, let $p(x)$ $(x \in R)$ be its associated probability density function (*pdf*). If f: $R \rightarrow R$ is a smooth function of x, we recall that the expectation $Ef(X)$ of f is defined by

$$Ef(X) := \int f(x)p(x)dx \tag{2}$$

where the integration is taken over the entire domain of the *pdf*. The variance $Vf(X)$ is defined by

$$Vf(X) := E(f(X) - Ef(X))^2 \tag{3}$$

For brevity, we will sometimes write μ_x and σ_x^2 for the expectation and variance of the random variable X, respectively.

In the classical Monte Carlo method, we estimate $Ef(X)$ by

$$Ef(X) \approx \frac{1}{N}\sum_{i=1}^{N} f(x_i) \tag{4}$$

The N samples $x_1, \ldots, x_n$ are generated according to the probability density of X. The convergence of this estimate to $Ef(X)$ as $N \rightarrow \infty$ is guaranteed by the large number theorem (Shiryayev 1984; Ross 1997).

It is well known that the approximation error made using Eqn 4 is proportional to $\sqrt{Vf(X)}/\sqrt{N}$. For computationally intensive problems, this slow convergence rate might render the Monte Carlo approximation impractical. In our Results section, we will see the extent to which the sensitivity derivative Monte Carlo method alleviates this slow convergence.

Moments method

Let us again assume that f: $R \rightarrow R$ is a smooth function of the random variable X and that X has a given probability density function. In the moments method, the function $y = f(x)$ is expanded in a Taylor series about the expectation μ_x of X:

$$y = f(\mu_x) + f'(\mu_x)(x - \mu_x) + \frac{1}{2}f''(\mu_x)(x - \mu_x)^2 + O((x - \mu_x)^3) \tag{5}$$

Here the primes denote derivatives with respect to X. With only a minimal amount of effort, the moments method gives the following first-order approximations of the expectation μ_y and variance σ_y^2 of $y = f(x)$

$$\mu_y = f(\mu_x) + O(\sigma_x^2) \tag{6}$$

$$\sigma_y^2 = \sigma_x^2 f'(\mu_x)^2 + O(\sigma_x^3) \tag{7}$$

Sensitivity derivative enhanced sampling

Recently, Cao *et al*. (2003, 2004) developed a variance-reduction method that exploits information regarding the sensitivity of f with respect to the random variable X (measured via derivatives

of f with respect to X) to improve the convergence characteristics of the Monte Carlo method. The result of their efforts was the sensitivity derivative enhanced sampling method (SDES). The first-order SDES method is described below.

Under the tacit assumption that the appropriate derivatives of the function f exist, consider the first-order Taylor expansion of f about μ_x:

$$J_1(x) := f(\mu_x) + f'(\mu_x)(x - \mu_x) \tag{8}$$

Using

$$\int p(x)dx = 1 \quad \text{and} \quad \int (x - \mu_x)p(x)dx = 0$$

it is clear that

$$\int (f(x) - J_1(x))p(x)dx = \int f(x)p(x)dx - f(\mu_x)$$

On rearranging for $Ef(X)$, this suggests the sensitivity derivative Monte Carlo approximation of the expectation of f

$$Ef(X) \approx f(\mu_x) + \frac{1}{N}\sum_{i=1}^{N}(f(x_i) - J_1(x_i)) \tag{9}$$

The N samples are again generated according to the *pdf* of X.

The following inequalities illustrate the extent to which the variance of Eqn 9 is reduced compared with the variance of the traditional Monte Carlo expectation estimate Eqn 4. Let

$$m_1 = \max_{s\in R}|f'(s)| \quad \text{and} \quad m_2 = \max_{s\in R}|f''(s)|$$

Then

$$Vf(X) \le 2m_1^2 V(X) \tag{10}$$

$$V(f - J_1) \le \frac{m_2^2}{2}(V(X)^2 + E((X - \mu_x)^4)) \tag{11}$$

Eqns 10 and 11 indicate that the SDES method is most efficient when $V(X)$ is small. See Cao *et al*. (2006) for a rigorous proof of these results as well as a generalisation to the nth-order SDES method.

It must be emphasised that whereas the convergence rate of the Monte Carlo method depends on $\sqrt{Vf(X)}/\sqrt{N}$, the SDES convergence rate for the first-order case depends on $\sqrt{V(f - J_1)}/\sqrt{N}$, where the quantity $V(f - J_1)$ is simply the variance of the first-order Taylor remainder of the objective function. (Note that although the Monte Carlo and SDES estimates are formulated differently, they converge to the same quantity $Ef(X)$, albeit at different rates.) If the objective function satisfies certain smoothness properties, the variance of the Taylor remainder $V(f - J_1)$ is always less than that of the objective function $Vf(X)$ itself, leading to an order of magnitude faster convergence of SDES relative to that of the Monte Carlo method. For instance, suppose we are to perform a simulation using $n = 10\,000$ samples for both the Monte Carlo method and SDES. SDES is able to achieve an order of magnitude (factor of 10) greater accuracy (because it converges to the exact value faster) than the Monte Carlo method, because $V(f - J_1)$ is smaller than $Vf(X)$. For a given accuracy, SDES is found to require a factor of 10 fewer samples than the standard Monte Carlo method. If the SDES is coupled with another variance reduction procedure such as stratified sampling, a reduction in the number of samples of up to two orders of magnitude can be achieved.

SDES and the Rothermel model

Although in the present article we concentrate our efforts on the Rothermel model, we will state the mathematical model as a general non-linear system of equations. The SDES method is applicable to any fire behaviour model satisfying the appropriate smoothness assumptions.

Let the vector $X = (X_1, \ldots, X_m)$ represent the ensemble of input parameters that comprise the local fire environment and suppose $y = f(X)$ is a function of the random variable vector X. Here y may represent the effective wind speed *efw*, the maximum rate of spread *ros*, or the spread direction *sdr*. The vector X is composed of the fuel type, fuel moisture, terrain, and weather parameters. We shall denote the expectation of the parameter vector X by $\mu_x = (\mu_x, \ldots, \mu_{x_m})$ and the covariance of X by Σ. In this case, the second-order SDES method is given by:

$$Ef(X) \approx \frac{1}{N}\sum_{i=1}^{N}(f(x_i) - J_2(x_i)) + f(\mu_x) + \frac{1}{2}\text{trace}(\nabla^2 f(\mu_x)\Sigma) \tag{12}$$

where

$$J_2(x) = f(\mu_x) + \nabla f(\mu_x)(x - \mu_x) + \frac{1}{2}(x - \mu_x)^T \nabla^2 f(\mu_x)(x - \mu_x)$$

Here ∇f and $\nabla^2 f$ denote the gradient and Hessian of f.

SDES coupled with stratified sampling

To further improve the efficiency of our sampling methods, we couple SDES with stratified sampling. The standard stratified sampling technique is developed below.

Let Φ represent the cumulative distribution function (*cdf*) of the random variable X with associated probability density function p; then

$$\Phi(x) := \int_{-\infty}^{x} p(s)ds \tag{13}$$

Notice that Φ is a non-decreasing function with range [0,1]. In stratified sampling, we divide the interval [0,1] into K strata (not necessarily of equal length):

$$[\omega^k, \omega^{k+1}] \ (k = 0, 1, \ldots, K - 1)$$

where

$$\omega^k = \frac{k}{K} \ (k = 0, 1, \ldots, K - 1)$$

Then, for each stratum k, we choose N_k random samples $u_1^k, \ldots, u_{N_k}^k$, uniformly distributed in the interval $[\omega^k, \omega^{k+1}]$. Next, we use the inverse *cdf* of X to generate N_k new samples $x_1^k, \ldots, x_{N_k}^k$ distributed according to the *pdf* of X:

$$x_i^k = \Phi^{-1}(u_i^k) \ (i = 1, \ldots, N_k)$$

A Monte Carlo estimate of the expectation of a function f: $R \rightarrow R$ of a random variable X can now be computed as

$$Ef(X) \approx \frac{1}{K}\sum_{k=0}^{K-1}\left(\frac{1}{N_k}\sum_{i=1}^{N_k} f(x_i^k)\right) \tag{14}$$

Similarly, to couple the first-order SDES and stratified sampling, we proceed as follows:

$$Ef(X) \approx \frac{1}{K}\sum_{k=0}^{K-1}\left(f(\mu_x^k) + \frac{1}{N_k}\sum_{i=1}^{N_k}(f(x_i^k) - J_1^k(x_i^k))\right) \tag{15}$$

where

$$J_1^k(x) := f(\mu_x^k) + f'(\mu_x^k)(x - \mu_x^k) \tag{16}$$

and μ_x^k denotes the expectation of X in the kth stratum and is given by

$$\mu_x^k = \frac{\int_{\omega^k}^{\omega^{k+1}} sp(s)ds}{\int_{\omega^k}^{\omega^{k+1}} p(s)ds} \quad (k = 0, 1, \ldots, K-1) \tag{17}$$

In the case of a normal distribution, the integral in the numerator can be computed analytically. The denominator can be calculated using numerical software that approximates the cumulative distribution function. It is worth emphasising that coupling stratified sampling with SDES makes even greater use of sensitivity derivatives. Whereas a first-order SDES uses only one set of derivatives (evaluated at μ_x), stratified sampling takes advantage of a set of K derivatives (evaluated at $\mu_x^0, \ldots, \mu_x^{K-1}$).

A simple example

Before proceeding to the main results, we will illustrate the previous methods with a simple example. Consider the function

$$f(X) = e^X$$

where we take $X \sim N(\mu, \sigma^2)$ (i.e. X is a normally distributed random variable with mean μ and variance σ^2).

To form the classical Monte Carlo estimate of the expectation of f, we must first generate N samples $x_1, \ldots, x_N$ that are normally distributed with mean μ and variance σ^2. Next, we use Eqn 4 to find

$$Ef(X) \approx \frac{1}{N}\sum_{i=1}^{N} f(x_i) = \frac{1}{N}\sum_{i=1}^{N} e^{x_i}$$

We may use the same N samples $x_1, \ldots, x_N$ and Eqn 9 to form the first-order SDES estimate of the expectation of f

$$\begin{aligned} Ef(X) &\approx f(\mu) + \frac{1}{N}\sum_{i=1}^{N}[f(x_i) - J_1(x_i)] \\ &= e^{\mu} + \frac{1}{N}\sum_{i=1}^{N}[e^{x_i} - (e^{\mu} + e^{\mu}(x_i - \mu))] \end{aligned}$$

The second-order SDES estimate is formed similarly.

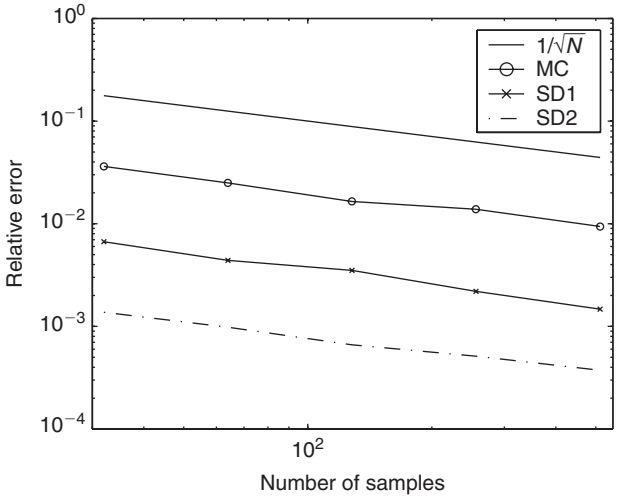

Fig. 1. Monte Carlo *v.* sensitivity derivative enhanced sampling method (SDES). Log-log plot of the average relative errors in the L_2-norm using $N = 32, 64, \ldots, 1024$ samples. Top solid line $= 1/\sqrt{N}$, Monte Carlo = MC, first-order SDES = SD1, second-order SDES = SD2. The average is taken over 120 sets of different samples. Here $f(X) = e^X$ where X is normally distributed with mean $\mu = 1/2$ and variance $\sigma^2 = 1/16$.

Because X is normally distributed, the probability density function is given by

$$p(x) = \frac{1}{\sqrt{2\pi\sigma^2}} e^{-\frac{(x-\mu)^2}{2\sigma^2}}$$

with domain $(-\infty,\infty)$. Performing the integration Eqn 2, the exact value of the expectation is

$$\begin{aligned} Ef(X) &= \int_{-\infty}^{\infty} e^x p(x)dx = \frac{1}{\sqrt{2\pi\sigma^2}}\int_{-\infty}^{\infty} e^x e^{-\frac{(x-\mu)^2}{2\sigma^2}} dx \\ &= e^{\frac{1}{2}\sigma^2+\mu} \end{aligned}$$

Fig. 1 illustrates the average relative errors using the L_2-norm (more on this later) with $N = 32, 64, \ldots, 1024$. To produce the plots above, 120 different sample sets per sample are used. Notice the substantial improvement of nearly two orders of magnitude in the convergence characteristics using the second-order SDES over the traditional Monte Carlo method.

Results and discussion

Because the main functions of interest, the rate of spread and the effective wind speed, depend on 15 variables or more, it is not possible to generate meaningful plots of these functions without making some simplifications. However, some representative plots of the rate of spread and the effective wind speed have been included (see Figs 2 and 3); in these figures, all input variables save two – the fuel bed depth d and the surface-area-to-volume ratio sv_{d1} – are set to a constant mean value.

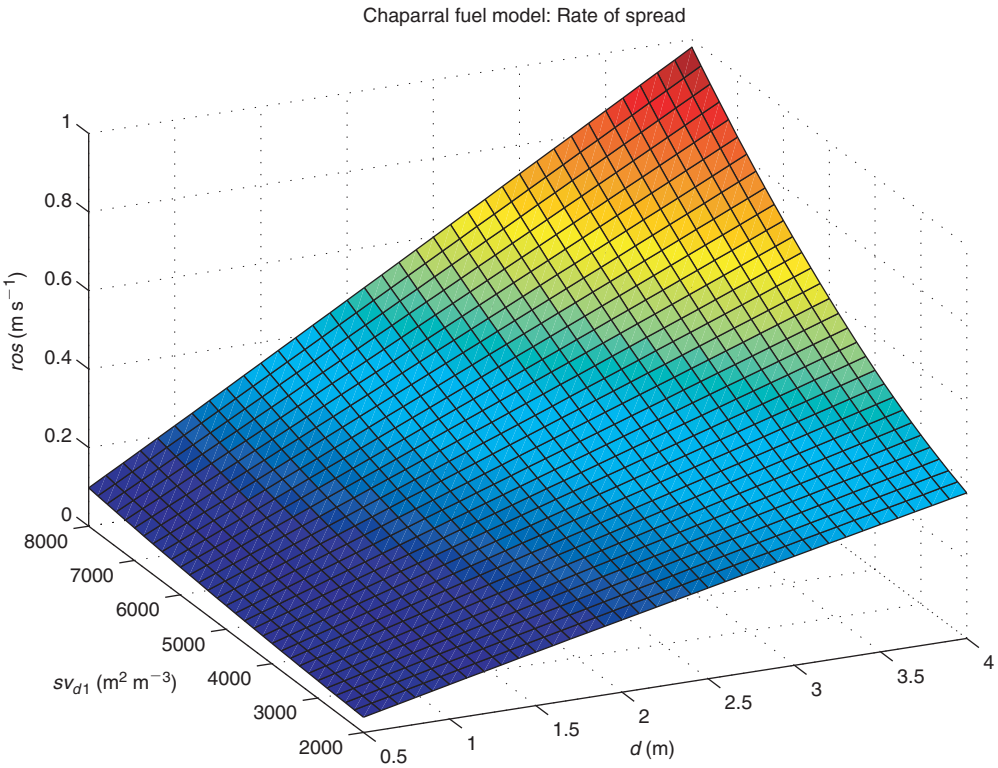

Fig. 2. Representative plot of the rate of spread (*ros*) using the Chaparral fuel model with all parameters, except d and sv_{d1}, set to the constant mean values indicated in Table 1.

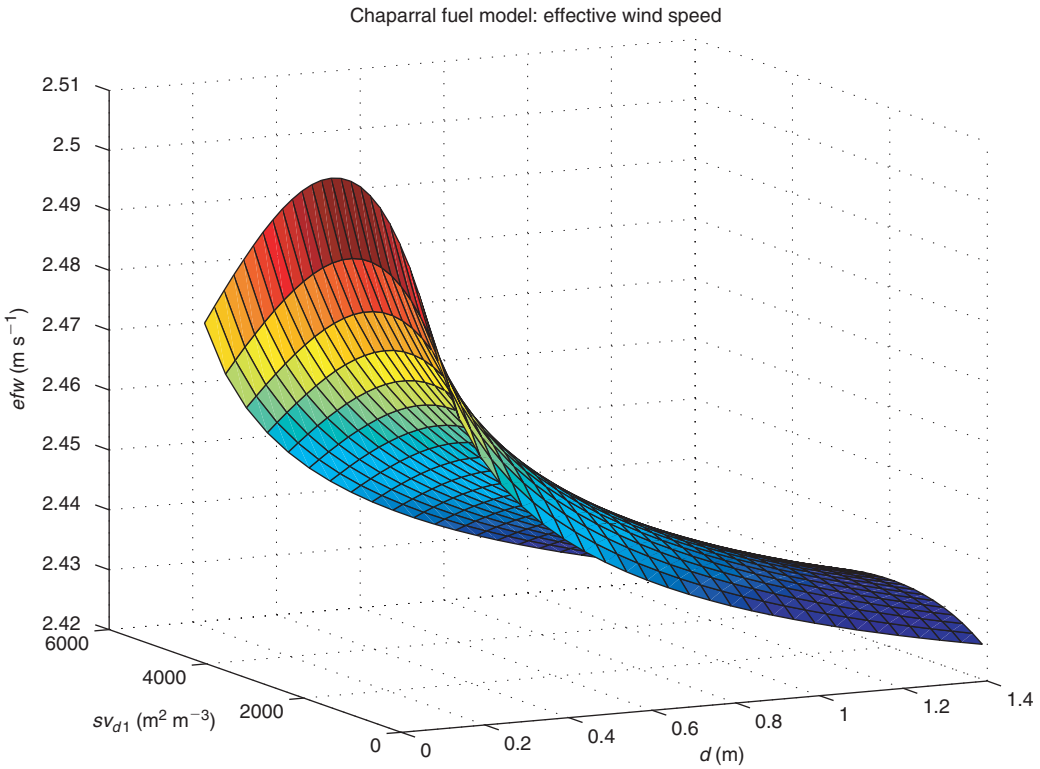

Fig. 3. Representative plot of the effective wind speed (*efw*) using the Chaparral fuel model with all parameters, except d and sv_{d1}, set to the constant mean values indicated in Table 1.

To compare the efficiency of SDES with traditional Monte Carlo methods, we compute the rate of spread *ros*, effective wind speed *efw*, and the spread direction *sdr* using two of the original fuel models found in Rothermel (1972): the short-grass and chaparral fuel models. The main fuel parameters are summarised in Tables 1 and 2. The following parameters are held constant throughout for both fuel models: the dead fuel moisture 8%, the live fuel moisture 150%, and the low heat content $18\,622\,\mathrm{kJ\,kg^{-1}}$. We shall also examine the additional speed-up obtained by coupling SDES with standard stratified sampling.

The uncertainty associated with an input parameter is described by assigning it a normal distribution with a typical mean (taken to be the value given in the original model) and a corresponding standard deviation (typically between 10 and 50% of the mean value). Two types of computations will be performed for each fuel model. First, we take the fuel bed depth d and the 1-h surface-area-to-volume ratio sv_{d1} to be normally distributed random variables; all other parameters are fixed. Then, we include a random wind speed *wsp* and wind direction θ in addition to d and sv_{d1}.

To measure improvement ratios of Monte Carlo approximations *v.* SDES, we use the L_2-norm (Euclidean distance). Recall that the L_2-norm is defined for a vector $x=(x_1,\ldots,x_n)$ as $\|x\|_2=(x_1^2+\cdots+x_n^2)^{1/2}$. If $E^{MC}=(E_1^{MC},\ldots,E_M^{MC})$ is a sequence of relative errors obtained from M Monte Carlo simulations, then a measure of the average error is given by:

$$\|E^{MC}\|_2=\left(\frac{1}{M}\sum_{i=1}^{M}[E_i^{MC}]^2\right)^{1/2}$$

To compute the relevant errors, we take the 'exact' expected value to be the Monte Carlo estimate using 250 sets of ~32 000 samples each. The L_2 improvement ratio is computed from:

$$I_2=\frac{\|E^{MC}\|_2}{\|E^{SDES}\|_2}$$

Table 1. Chaparral fuel model parameters

Parameter	Symbol	μ	σ	Units
1-h fuel load	$w0_{d1}$	1.12	–	$\mathrm{kg\,m^{-2}}$
10-h fuel load	$w0_{d2}$	0.90	–	$\mathrm{kg\,m^{-2}}$
100-h fuel load	$w0_{d3}$	0.45	–	$\mathrm{kg\,m^{-2}}$
Live herbaceous fuel load	$w0_{lh}$	0.0	–	$\mathrm{kg\,m^{-2}}$
Live woody fuel load	$w0_{lw}$	1.12	–	$\mathrm{kg\,m^{-2}}$
1-h surface area/volume ratio	sv_{d1}	6562	740	$\mathrm{m^2\,m^{-3}}$
Live herb surface area/volume ratio	sv_{lh}	4921	–	$\mathrm{m^2\,m^{-3}}$
Live woody surface area/volume ratio	sv_{lw}	4921	–	$\mathrm{m^2\,m^{-3}}$
Dead fuel moisture of extinction	*mx*	20	–	%
Fuel bed depth	*d*	1.83	0.3	m
Slope	*slp*	14.04	–	degrees
Midflame wind speed	*wsp*	2.3	0.5	$\mathrm{m\,s^{-1}}$
Direction of wind vector (from upslope)	θ	45	20	degrees

Table 2. Short-grass fuel model parameters

Parameter	Symbol	μ	σ	Units
1-h fuel load	$w0_{d1}$	0.17	–	$\mathrm{kg\,m^{-2}}$
10-h fuel load	$w0_{d2}$	0.0	–	$\mathrm{kg\,m^{-2}}$
100-h fuel load	$w0_{d3}$	0.0	–	$\mathrm{kg\,m^{-2}}$
Live herbaceous fuel load	$w0_{lh}$	0.0	–	$\mathrm{kg\,m^{-2}}$
Live woody fuel load	$w0_{lw}$	0.01	–	$\mathrm{kg\,m^{-2}}$
1-h surface area/volume ratio	sv_{d1}	11 483	1150	$\mathrm{m^2\,m^{-3}}$
Live herb surface area/volume ratio	sv_{lh}	4921	–	$\mathrm{m^2\,m^{-3}}$
Live woody surface area/volume ratio	sv_{lw}	4921	–	$\mathrm{m^2\,m^{-3}}$
Dead fuel moisture of extinction	*mx*	12	–	%
Slope	*slp*	14.04	–	degrees
Fuel bed depth	*d*	0.30	0.05	m
Midflame wind speed	*wsp*	2.3	0.5	$\mathrm{m\,s^{-1}}$
Direction of wind vector (from upslope)	θ	45	20	degrees

Table 3. Average improvement ratios for first moment estimates of the rate of spread using first-order sensitivity derivative enhanced sampling method (SDES) with four strata *v*. Monte Carlo (improvement ratio denoted by I_{MC}). Improvement ratio using only stratified sampling with four strata *v*. Monte Carlo (improvement ratio denoted by I_{S4})
Here $N = 32, 64, \ldots, 1024$ and $M = 100$ different sets of samples

Fuel model	I_{MC} (2 vars)	I_{MC} (4 vars)	I_{S4} (2 vars)	I_{S4} (4 vars)
Chaparral	37.2	5.6	13.5	2.8
Short grass	24.2	4.3	10.0	3.1

Table 4. Timing results (in seconds)
Average computational time comparison of Monte Carlo (MC) *v*. first-order sensitivity derivative enhanced sampling method (SDES) coupled with stratified sampling with four strata (SSD1)

N	(Chap)MC	(Chap)SSD1	(Shtgrs)MC	(Shtgrs)SSD1
32	4.297×10^{-2}	4.437×10^{-2}	4.063×10^{-2}	4.344×10^{-2}
64	8.188×10^{-2}	8.250×10^{-2}	7.922×10^{-2}	8.250×10^{-2}
128	1.617×10^{-1}	1.656×10^{-1}	1.567×10^{-1}	1.566×10^{-1}
256	3.231×10^{-1}	3.295×10^{-1}	3.113×10^{-1}	3.158×10^{-1}
512	6.423×10^{-1}	6.255×10^{-1}	6.216×10^{-1}	6.262×10^{-1}

Suppose, for example, that we use a Monte Carlo and a first-order SDES simulation to approximate the rate of spread using 5000 samples. If the improvement ratio is $I_2 = 10$, then this says that the average relative error obtained from SDES is 10 times smaller than that obtained from a Monte Carlo method using the same number of samples. Put another way, if we use SDES, we need only 500 samples to achieve the same accuracy as the Monte Carlo method.

Table 5. Chaparral fuel model summary results using the four random variables: *d*, fuel bed depth; sv_{d1}, 1-h surface area/volume ratio; *wsp*, midflame wind speed; and direction of wind vector (from upslope) θ using sensitivity derivative enhanced sampling method (SDES) coupled with four strata
$N = 1024$ samples using $M = 100$ different sample sets

Parameter	Symbol	μ	σ	Units
Effective wind speed	*efw*	2.41	7.39×10^{-6}	$m\,s^{-1}$
Rate of spread	*ros*	0.353	1.02×10^{-4}	$m\,s^{-1}$
Spread direction	*sdr*	41.3	1.71×10^{-4}	degrees

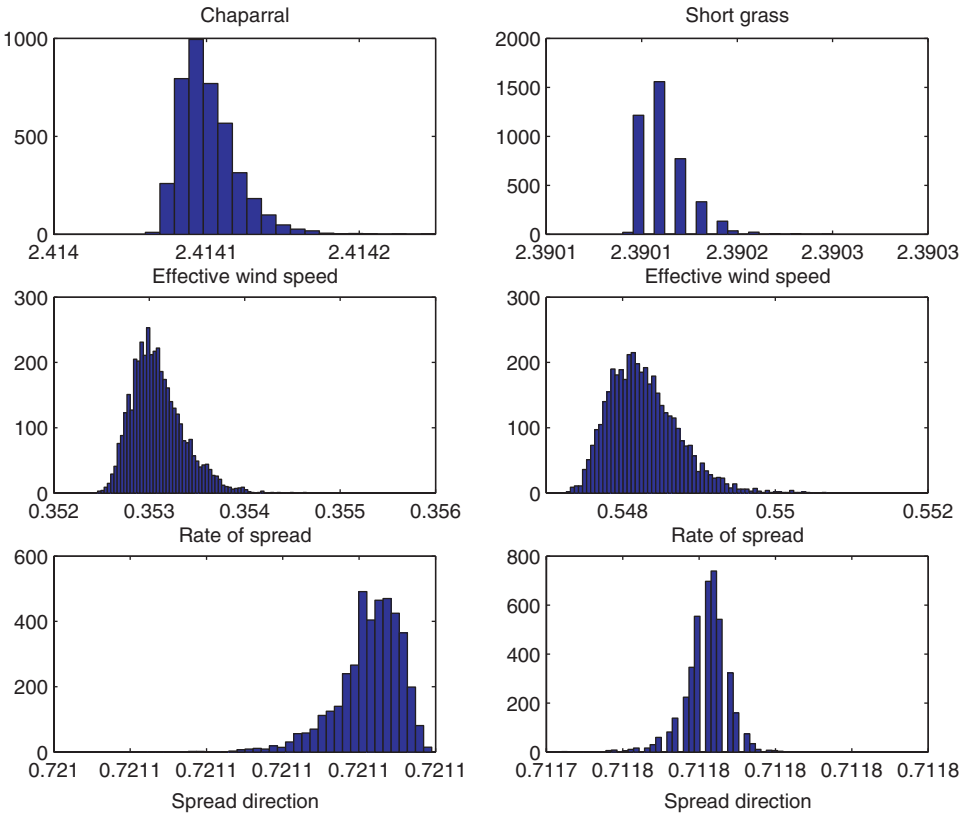

Fig. 4. Histograms of the effective wind speed, rate of spread, and spread direction using four random variables: fuel bed depth, 1-h surface area/volume ratio, midflame wind speed and direction of wind vector denoted by d, sv_{d1}, *wsp* and θ respectively. In all cases, the ordinate denotes the frequency (number of samples). The mean values for the Chaparral fuel model are given by $efw_\mu = 2.41\ m\,s^{-1}$ (mean effective wind speed), $ros_\mu = 0.353\ m\,s^{-1}$ (mean rate of spread) and $sdr_\mu = 41.3°$ (mean spread direction).

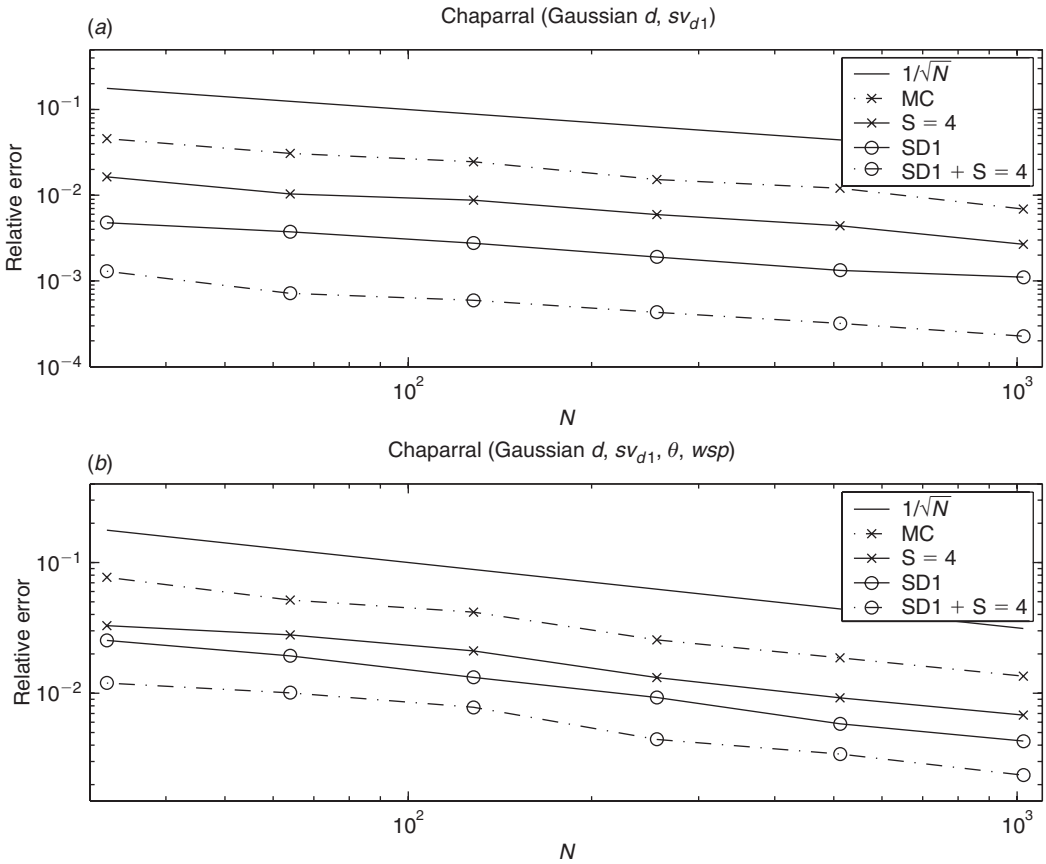

Fig. 5. (Chaparral fuel model) Average relative errors in first moment estimates for the rate of spread *ros* ($m\,s^{-1}$) using (*a*) two random variables $sv_{d1} \sim N(6562, 740)$ ($m^2\,m^{-3}$) and $d \sim N(1.83, 0.3)$ (m); and (*b*) four random variables $sv_{d1} \sim N(6562, 740)$ ($m^2\,m^{-3}$), $d \sim N(1.83, 0.3)$ (m), $wsp \sim N(2.3, 0.5)$ ($m\,s^{-1}$) and $\theta \sim N(45, 20)$ (degrees).

Table 3 shows that even with a simple first-order SDES method, the convergence gain over a traditional Monte Carlo simulation can be more than 30 times faster. Notice that as $I_{MC} = 24.2$ when we consider the short grass fuel model using two random variables (namely d and sv_{d1}), this implies that, on average, it takes the Monte Carlo method approximately 24 times the number of samples to achieve the same accuracy as a first-order SDES coupled with stratified sampling (four strata).

It is important to note that SDES might require the computation of several derivatives of the objective function. In our computations, an automatic differentiation package (Stamatiadis *et al*. 2000) was used to find the relevant derivatives and Table 4 illustrates that even when we couple SDES with stratified sampling (denoted by SSD1, for a first-order SDES with stratified sampling), the extra computational expense incurred is marginal.

Fig. 4 illustrates that although the input parameters follow a normal distribution, this is not the case with the output functions *efw*, *ros* and *sdr*. This is to be expected, as the output functions depend non-linearly on the random parameters. Using four random variables in the chaparral fuel model, the mean values are given by $efw_\mu = 2.41\,m\,s^{-1}$, $ros_\mu = 0.353\,m\,s^{-1}$, and $sdr_\mu = 41.3°$. The corresponding standard deviations are $efw_\sigma = 7.39 \times 10^{-6}\,m\,s^{-1}$, $ros_\sigma = 1.02 \times 10^{-4}\,m\,s^{-1}$, and $sdr_\sigma = 1.71 \times 10^{-4}$ (see Table 5 for a summary of the results). The standard deviation provides us with a measure of the uncertainty in the outputs.

Figs 5, 6 and 7 show that the relative errors decay at the theoretically expected rate proportional to $1/\sqrt{N}$, where N is the number of samples used. For the chaparral fuel, sample sets range from $N = 32, 64, 128, \ldots,$ to 1024 samples per set. Throughout, we use $M = 100$ different sets of samples and then average the relative errors. Fig. 5*a* depicts the first-moment estimate (mean value) of the rate of spread using only two Gaussian random variables $d \sim N(1.83, 0.3)$ and $sv_{d1} \sim N(6562, 740)$. Observe that, in this case, stratified sampling is as much as five times faster than the traditional Monte Carlo method. The improvement in convergence when first-order SDES is coupled with stratified sampling (using four strata) is even more dramatic. This time, the estimate is approximately two orders of magnitude more accurate than that obtained with the traditional Monte Carlo method. Equivalently, for a given accuracy, it would take the Monte Carlo method as many as 100 times more samples to achieve comparable results.

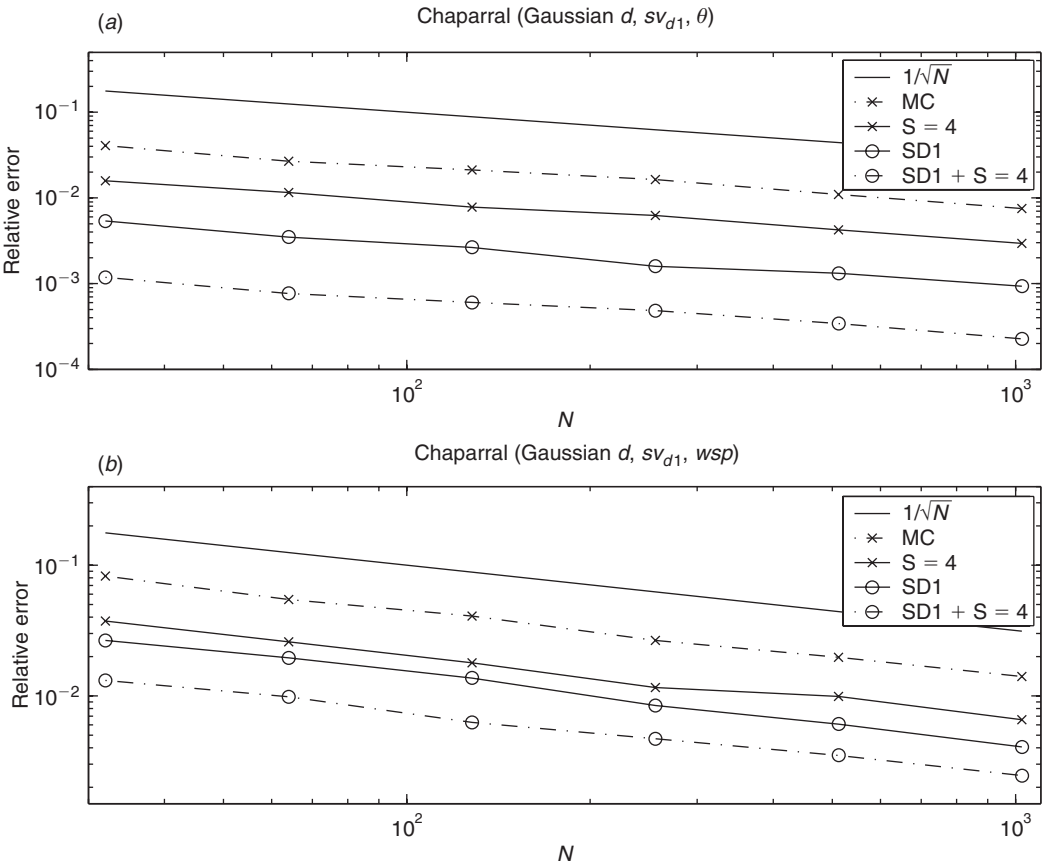

Fig. 6. (Chaparral fuel model) Average relative errors in first moment estimates for the rate of spread *ros* ($m\,s^{-1}$) (*a*) using the random variables $d \sim N(1.83, 0.3)$ (m), $sv_{d1} \sim N(6562, 740)$ ($m^2\,m^{-3}$), $\theta \sim N(45, 20)$ (degrees); and (*b*) using the random variables $d \sim N(1.83, 0.3)$ (m), $sv_{d1} \sim N(6562, 740)$ ($m^2\,m^{-3}$), $wsp \sim N(2.3, 0.5)$ ($m\,s^{-1}$). Here $N = 32, 64, \ldots, 1024$ and $M = 100$.

However, Fig. 5*b* illustrates that the acceleration gains are more modest when we consider the four random variables *d*, sv_{d1}, θ and *wsp*. As the improved convergence takes a toll with the addition of the random parameters θ, the wind direction relative to the upslope direction, and the wind speed *wsp*, we investigate the impact each has on the first-moment estimate individually. It is evident from Fig. 6 that the SDES convergence improvement is of the same order with *d*, sv_{d1} and θ as when we consider only *d* and sv_{d1}. The convergence, however, deteriorates when the wind speed *wsp* is included as an additional parameter along with *d* and sv_{d1}. As SDES exploits the sensitivity of the object function (in this case *ros*) with respect to its parameters (measured via derivatives of the function) to generate a more efficient estimate of the expectation, we should observe a more substantial improvement in the convergence whenever the object function is highly sensitive to the given parameter. Thus, the results in Fig. 6 can be restated by saying that, with the given mean values, the rate of spread is more sensitive to changes in wind direction than to changes in wind speed. The importance of the wind direction relative to the upslope direction is not surprising as this is effectively how Rothermel couples with different modes of heat transfer. Because this relative wind direction is so important in the Rothermel model, it stresses the need for detailed descriptions of topography and winds across the landscape to minimise this source of uncertainty.

The short-grass fuel model, with $M = 100$ sample sets and $N = 32, \ldots, 512$ samples each (Fig. 7), exhibits a similar convergence phenomenon. A reduced SDES convergence is evident when we consider the four random variables *d*, sv_{d1}, θ and *wsp* instead of just *d* and sv_{d1}. Nevertheless, first-order SDES coupled with stratified sampling still results in a convergence that is nearly 10 times faster than the traditional Monte Carlo method.

Conclusions

The simplicity of the Monte Carlo method makes it an attractive method in simulations where fire spread models such as the Rothermel model are used. However, its slow convergence can render its application infeasible especially in time-sensitive situations such as in the prediction of an ongoing fire. In the present work, we propose sensitivity derivative enhanced sampling (SDES), which offers fire researchers an economic alternative to traditional Monte Carlo methods to quantify parametric uncertainty. The speed-up of approximately an order of

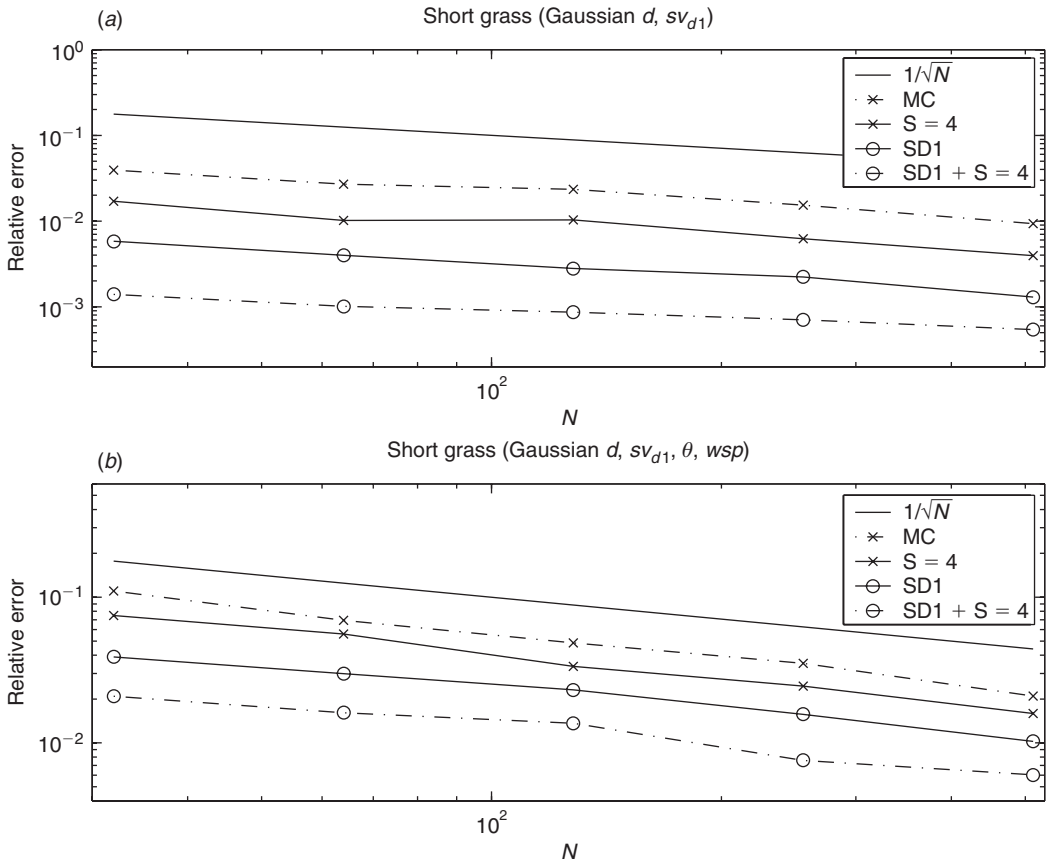

Fig. 7. (Short grass fuel model) Average relative errors in first moment estimates for the rate of spread *ros* ($m\,s^{-1}$) using (*a*) two random variables $sv_{d1} \sim N(11\,483,\ 1150)$ ($m^2\,m^{-3}$) and $d \sim N(0.030,\ 0.05)$ (m); and (*b*) four random variables $sv_{d1} \sim N(11\,483,\ 1150)$, $d \sim N(0.030,\ 0.05)$, $wsp \sim N(2.3,\ 0.5)$ ($m\,s^{-1}$) and $\theta \sim N(45,\ 20)$ (degrees).

magnitude gained by using first-order SDES over Monte Carlo with the fuel models considered is encouraging. The results further indicate that coupling SDES with stratified sampling can further accelerate the convergence. When coupled with stratified sampling, an improvement of nearly two orders of magnitude could spell the difference between running a simulation for 10 h using the Monte Carlo method or 6 min with a first-order SDES. It is clear that this relatively simple method endows fire managers with the ability to run simulations efficiently, perhaps in real time, while requiring only modest computational resources.

Coupling SDES with more sophisticated sampling techniques such as Latin hypercube sampling or orthogonal sampling may improve the convergence rate even further. We will explore these possible enhancements in future investigations. SDES can also serve as a dual-purpose tool that can help identify those parameters to which the object function is most sensitive. Understanding the impact of parametric uncertainty is of paramount importance as key input parameters are seldom known exactly. In some situations, it may be unnecessary to obtain a precise measurement of a given parameter as the function, such as the rate of spread, may largely be unaffected for a wide range of values.

Although one of the primary goals of the current work was to demonstrate that it is computationally feasible to estimate the impact of parametric uncertainty using the Rothermel model, the long-term practical applications of uncertainty quantification to fire models are numerous. Although a single application of the Rothermel model might generate an erroneous prediction of the rate of spread because of, say, unreliable (uncertain) fuel data, knowledge of the distribution of the fuel data (which can be estimated if sufficient sample measurements are taken) can be exploited to estimate the distribution of the rate of spread. An estimated distribution of the rate of spread can be more useful than a single prediction because not only can the average rate of spread be computed, but an associated measure of uncertainty via confidence intervals can also be assigned to it as well. A fire manager who must prioritise the allocation of limited resources can use the statistical information gained from an uncertainty analysis to distribute resources optimally.

The important question of how parametric variance might affect multiple spatiotemporal evolutionary calculations using a fire growth simulation system such as *FARSITE*, and the effect this might have on the averaging of randomly distributed errors generated by the instantaneous sampling of the Rothermel formulae will be addressed in future research.

References

Bachmann A (2001) GIS-based wildland fire risk analysis. PhD thesis, Universität Zürich, Switzerland.

Bachmann A, Allgower B (2002) Uncertainty propagation in wildland fire behaviour modeling. *International Journal of Geographical Information Science* **16**, 115–127. doi:10.1080/13658810110099080

Cao Y, Hussaini MY, Zang TA (2003) An efficient Monte Carlo method for optimal control problems with uncertainty. *Computational Optimization and Applications* **26**, 219–230. doi:10.1023/A:1026079021836

Cao Y, Hussaini MY, Zang TA (2004) Exploitation of sensitivity derivatives for improving sampling methods. *AIAA Journal* **42**, 815–822. doi:10.2514/1.2820

Cao Y, Hussaini MY, Zang TA, Zatezalo A (2006) A variance reduction method based on sensitivity derivatives. *Applied Numerical Mathematics* **56**, 800–813. doi:10.1016/J.APNUM.2005.06.010

Cova TJ, Dennison PE, Kim TH, Moritz MA (2005) Setting wildfire evacuation trigger points using fire spread modeling and GIS. *Transactions in GIS* **9**, 603–617. doi:10.1111/J.1467-9671.2005.00237.X

Deeming JE, Burgan RE, Cohn JD (1978) The National Fire Danger Rating System. USDA Forest Service, Intermountain Forest and Range Experiment Station, General Technical Report INT-39. (Ogden, UT)

Finney MA (1998) *FARSITE*: Fire Area Simulator – model development and evaluation. USDA Forest Service, Rocky Mountain Station, Research Paper RMRS-RP-4. (Fort Collins, CO)

Fujioka FM (2002) A new method for the analysis of fire spread modeling errors. *International Journal of Wildland Fire* **11**, 193–203. doi:10.1071/WF02004

Mathelin L, Hussaini MY, Zang TA, Bataille F (2004) Uncertainty propagation for a turbulent, compressible nozzle flow using stochastic methods. *AIAA Journal* **42**, 1669–1676. doi:10.2514/1.5674

McArthur AG (1966) Weather and grassland fire behaviour. Department of National Development, Forestry and Timber Bureau, Forestry Research Institute, Leaflet No. 100. (Canberra, ACT)

Ross S (1997) 'A First Course in Probability.' (Prentice-Hall: Upper Saddle River, NJ)

Rothermel RC (1972) A mathematical model for predicting fire spread in wildland fuels. USDA Forest Service, Intermountain Forest and Range Experiment Station, Research Paper INT-115. (Ogden, UT)

Saltelli A, Tarantola S, Campolongo F, Ratto M (2004) 'Sensitivity Analysis in Practice: a Guide to Assessing Scientific Models.' (Halsted Press: New York)

Shiryayev AN (1984) 'Probability.' (Springer-Verlag: New York)

Stamatiadis S, Prosmiti R, Farantos SC (2000) Auto_deriv: tool for automatic differentiation of a FORTRAN code. *Computer Physics Communications* **127**, 343–355. doi:10.1016/S0010-4655(99)00513-5

Walters RW, Huyse L (2002) Uncertainty analysis for fluid mechanics with applications. ICASE Report No. 2002–1. (Hampton, VA)

Weber RO (2001) 'Wildland Fire Spread Models in Forest Fires: Behavior and Ecological Effects.' (Academic Press: San Diego, CA)

Manuscript received 16 May 2007, accepted 6 February 2008